



## EFFECTS OF HIGH LEVEL OF LEAD (II) OXIDE (PbO) USAGE ON ACCUMULATOR AND RESPONSE SURFACE METHOD

Emrah PIÇAKÇI<sup>1</sup>, Zehra Gülten YALÇIN<sup>1\*</sup>


<sup>1</sup>Karatekin University, Faculty of Engineering, Department of Chemical Engineering, 18200, Çankırı, Türkiye


**Abstract:** This study involved the preparation of lead oxide paste for use in the production of lead-acid batteries. The paste was applied to the positive plates, and its performance effects were tested on the battery. Morphological and surface area analyses were conducted using SEM and BET, respectively, after the performance tests. Two mixtures of lead oxide ratios, 25%Pb-75%PbO (sample A) and 30% Pb-70% PbO (sample B), were used. The dough was applied to positive grids and passed through the curing process. SEM images revealed that tribasic sulfate (3BS) structures had a higher charge acceptance rate than tetrabasic sulfate (4BS) structures. BET analyses showed that the surface area of the samples with A ratio was higher than that of B. Electrical tests were conducted in the laboratory, and the A sample was found to be 12% more effective in the first charging efficiency than the B sample. Sample A was also found to be 67% more efficient in charge acceptance tests and 6.5% more efficient in cycle tests. The study also showed that increasing the %Pb ratio in the product decreases the initial charge efficiency, charge acceptance, and cycle life. Finally, the response surface method was used to examine the 2D picture of the relationship between lead percentage and yield, and it was found that the highest yield was obtained at 26% lead yield, with the yield being inversely proportional to the increase in lead percentage, likely due to the effect of particle size and surface area.

**Keywords:** Lead (II) oxide, Lead acid battery, Positive plate, Performance tests, Surface response system

\*Corresponding author: Karatekin University, Faculty of Engineering, Department of Chemical Engineering, 18200, Çankırı, Türkiye

E mail: zaltin@karatekin.edu.tr (Z. G. YALÇIN)

Emrah PIÇAKÇI  <https://orcid.org/0000-0002-7552-439X>

Zehra Gülten YALÇIN  <https://orcid.org/0000-0001-5460-289X>

Received: June 21, 2023

Accepted: August 23, 2023

Published: October 15, 2023

Cite as: Piçakçı E, Yalçın ZG. 2023. Effects of high level of lead (II) oxide (PbO) usage on accumulator and response surface method. BSJ Eng Sci, 6(4): 375-386.

### 1. Introduction

A battery is a device that transforms chemical energy directly into electrical energy through an electrochemical oxidation-reduction reaction, which can be reversed in rechargeable systems. This reaction involves the transfer of electrons between materials through an electrical circuit. Unlike non-electrochemical redox reactions, where only heat is affected, batteries offer high energy conversion. There are several types of batteries classified according to the metal types used, such as lead-acid, nickel-cadmium, nickel-iron, nickel-metal hydride, lithium-ion, and silver-zinc batteries. Lead-acid batteries are the most commonly used due to their durability, low cost, well-understood electrochemistry, and high recyclability. These batteries can be classified as dry or wet. The advantages and disadvantages of the lead acid battery are as follows; Gutiérrez et al. (2018); Bode (1979); Bode (1977); Eydemir (2019); (Piçakçı et al. 2021).

#### 1.1. Advantages

- It is low cost.
- It is easy to recycle.
- It can be produced easily in high quantities.
- Recharge efficiency is high (>70%)
- Various sizes and capacity production are easy to

design.

- It is easily available in the market.

#### 1.2. Disadvantages

- Low cycle compared to other accumulators (Approximately 500 deep discharge-charge cycles).
- Low energy density (30-40 Wh/kg)
- Sulfation problem occurs when there is no long-term use.
- Flooded batteries

Starter batteries, also known as SLI (defined by the words starting, lighting, and ignition) batteries, are the most commonly used battery types. Automobiles, trucks, tractors etc. used in the fields Garcke (1990); Pavlov (2011).

#### 1.3. Dry batteries (VRLA)

The technological infrastructure of dry batteries differs from that of wet batteries, as dry batteries are classified into two categories: AGM (Absorbent Glass Mat) and gel batteries. Unlike wet batteries, dry batteries do not contain liquid electrolytes. As a result, they eliminate the risk of electrolyte leakage and overflow, which is often a concern with flooded batteries. Additionally, dry batteries produce significantly less gas than their wet counterparts, which leads to a longer shelf life and enhanced safety (Mitchell et al., 2009; Lu et al., 2022).

The scientific literature contains numerous studies



investigating the effects of various additives on the properties of positive and negative electrodes in lead acid batteries, with the goal of enhancing battery performance. In these studies, morphological analyses using SEM and BET were conducted to examine the impact of these additives on the positive plate dough, revealing notable structural changes (Wang et al., 1995; Lach et al., 2019; Jia et al., 2020).

The initial investigation of lead acid batteries by Mayer and Rand highlighted the crucial role of increasing the electrochemical reactivity of the active mass, which is one of many factors that can significantly impact battery performance. As researchers have noted, the production of lead oxide through mixing, hardening, and forming processes is a critical part of battery design and performance. The battery industry currently employs two primary methods for lead oxide production: the ball mill and Barton-pot processes. While both methods have their own unique advantages, it remains difficult to determine which yields the best lead oxide. Nevertheless, studies have emphasized that both the ball mill and Barton-pot products are effective in the production of automotive batteries. This study explores the current procedures for lead oxide production, the desirable properties of lead oxide, and the effect of this substance on battery performance (Mayer and Rand, 1996).

In a lead acid battery discharge lead sulfate is produced and it is also known that large  $PbSO_4$  crystals dissolve more slowly, thus causing the battery to fail. Little is known about the use of chemically prepared  $PbSO_4$  as the active ingredient in lead acid batteries.

Zhang et al. In their study, it is seen that they are working on the preparation of  $PbSO_4$  by chemically precipitating aqueous lead acetate with sodium sulfate and its use as a positive active material. In this study, it has been shown that  $PbSO_4$  alone is not sufficient for this, at different mixing ratios with  $Pb_3O_4$  at 5, 10, 20 and 30%, at a current density of 100 mA g<sup>-1</sup>, 78.2, 92.9, 88.0 and 91.5 It seems that the performance of mAh g<sup>-1</sup> has been reached. In addition, there is information that it remains at a capacity of 150 with 10%  $Pb_3O_4$ , and 93% at 100% battery charge (Zhang et al., 2016).

Zhang et al. In their study, the effects of expanded graphite, carbon fiber, needle odor and polyacene as positive electrode additives on the  $PbO_2$  electrode behavior of lead/acid batteries were investigated. It has been found that all additives can significantly increase the utilization coefficient of the positive active material during the first phase of the charge and discharge cycle (Zhang et al., 2017).

According to Liu et al. In their study, they investigated the effect and mechanism of iron-doped lead oxide on lead acid battery. Iron doped lead oxide has been found to significantly reduce battery capacity and cycle life, as well as promote the release of hydrogen and oxygen, resulting in poor performance of the iron "redox-diffusion" process. They seem to have concluded that  $PbSO_4$  formation causes poor performances (Liu et al.,

2011).

Bao et al. In their study, the mechanism of  $SiO_2+PbO_2$  powder as a positive electrode additive for lead-carbon batteries was investigated in detail. Silica and its compounds were tested for their electrochemical stability and strong electrolyte storage capacity in sulfuric acid solution. Since  $SiO_2+PbO_2$  has a high specific surface area and porous structure, it is seen that it gives good electrochemical performance at the anode. After these powders were added to the lead-carbon battery, this additive was found to increase ionic diffusion, creating extraordinary ion transfer channels within the positive active material (Bao et al., 2021).

According to Arun et al. In their study, it is seen that using standard production processes, lead acid batteries are formed on negative and positive plates containing two different carbon additives. They investigated the effects of morphological, porosity, BET surface area and battery performance in the dough plastered on the plates prepared with this additive. In the study conducted with carbon additives, it is seen that the effect on the discharge performance is positive. In addition, it was emphasized that the high surface area carbon additive increased the water loss and brought some disadvantages when adding it to the negative electrode (Arun et al., 2020).

Yin et al. conducted a study on lead-carbon anodes and proposed a novel approach using a carbon/lead (C/Pb) composite with electroless coating. The composite was found to reduce the hydrogen formation rate of the anode, protect its porous structure, and enhance the connection between the carbon and lead components. Additionally, the C/Pb composite was found to suppress hydrogen formation and incorporate carbon additives. The researchers highlighted the importance of reinforcing the connection between the components and the sponge lead material in their investigation (Yin et al. 2019).

Wang et al. In their study, they prepared new lead oxides with different particle sizes by the pyrolysis of lead citrate in a rotary kiln and investigated the mechanism of how the particle size affects the phase transition path of the new lead oxides during the wetting process.  $PbO$  with larger particle size (D50 diameter = 22.4  $\mu m$ ) converts to  $3PbO \cdot PbSO_4$ ,  $3PbO \cdot PbSO_4$  is then partially converted to  $PbO \cdot PbSO_4$  while  $PbO \cdot PbSO_4$  is gradually converted to  $PbSO_4$ . Smaller particle size  $PbO$  (D50 diameter = 8.3  $\mu m$ ) is directly converted to  $PbSO_4$ , and  $3PbO \cdot PbSO_4$  has been reported to be partially converted to  $PbO \cdot PbSO_4$ . Since  $PbO_2$  is the oxidation product of  $PbSO_4$  in the subsequent formation process, the phase compositions after soaking determined the  $PbO_2$  content in the positive plates. The particle size of leaded oxides determines the initial capacity of the test cells by affecting the wetting process, and it is stated that a linear correlation is obtained between the initial capacity in the positive plates and the  $PbO_2$  content (Wang et al., 2020).

Chen et al. (2013) emphasized that the microstructure

and surface morphology of lead dioxide ( $\text{PbO}_2$ ), as the positive active substance of the lead-acid battery, have a strong effect on the overall performance of the lead-acid battery. In this study, it is seen that a series of  $\text{PbO}_2$  thin films are produced on the pure Pb surface via Pb electrochemical oxidation. Its morphological effect and electrochemical properties were investigated. At the end of the study, it was found that the  $\text{PbO}_2$  layer formed had a high surface area, relatively small size, and especially higher discharge capacity and better cycling performance than other  $\text{PbO}_2$  layers. It is seen that micro/nano structured  $\text{PbO}_2$  materials improve their electrochemical performance (Chen et al., 2013; Yang et al., 2013).

Karimi et al. (2006) conducted a study aimed at enhancing the performance of lead-acid cells by improving their cycle life. In their research, they examined the use of sodium sulfate as an effective, low-cost additive for the negative paste in lead-acid batteries. The inclusion of sodium sulfate led to improvements in battery capacity, cold-start performance, and cycle life. The team carried out several practical production experiments using paste series with 0-4% of the new additive added to the negative active substances. Results showed that pastes containing sodium sulfate had significantly higher capacity, better cold-start performance, and longer cycle life than those without the additive.

According to Karimi et al. (2006) investigated the effect of sodium sulfate on the performance of sealed lead acid cells by using sodium sulfate at the positive electrode. It has found that the 4BS crystal size can be reduced in cured positive plates, thus providing a larger surface area that helps the user have better performance at high temperatures.

Kwiecien et al. (2018) in their study, they emphasized that sulphation affects the active surface area in the aging mechanisms of lead acid batteries. For this reason, it describes the accumulation of sulfate crystals on the surface of the electrodes in the reaction where corrosion resistance is also increased and spills occur. The low conductivity of the crystals results in local immobility with portions of inaccessible capacity as a result. The sulfate crystals are the product of the discharge reaction at both electrodes and are dissolved during the recharging process. It has been emphasized that the negative electrode is more exposed to sulfation due to its smaller surface area compared to the positive electrode. The response surface method is the experimental design method proposed by Kwiecien et al. (2018) in 1951. It is used to perform experiments and regressions on representative points available. It also determines the relationship between factors and outcomes in general terms (Dayton and Edwards, 2000). In the response surface method, it generates a regression that matches the equation of the process to be analyzed and estimates the value corresponding to each factor level by plotting the contour map. Response values of experimental conditions are determined separately for each factor.

Finally, a variable surface model is established through experiments to evaluate the factors affecting the results and their interactions.

Compared with traditional optimization methods, more accurate experimental results are obtained (Tong et al., 2015). In addition, it is necessary to apply various test methods in order to verify the created models. ANOVA analysis and the quality of fit of the results with the model equations were expressed using the coefficient of convergence ( $R^2$ ) (Zhang et al., 2017; Zhang et al., 2022). Researchers use the ( $R^2$ ) value to measure the accuracy of a model. The  $R^2$  adj value of the model is the modified version of the  $R^2$  coefficient. Adding factors that are known to have no effect on the model reduces the  $R^2$  adj value (Draper and Pukelsheim, 1996; Jensen, 2017). The response surface method can generally be divided into two stages. The first stage can be called the response surface design stage and the second stage can be called the response surface optimization stage. If there are many factors to be examined in the response surface design stage, screening experiments are performed to determine the importance of each factor and finally the factor with the greatest impact is selected for further investigation. Screening experiments include partial factorial design experiments. The main goal of the first phase is to examine the relationship between the current experimental conditions and the response surface. When test conditions are far from optimal, a first-order approximation model should be applied to the optimal location of the response surface (Sagbas, 2022; Elkelay et al., 2022; Kocakulak et al., 2023). The response surface method develops an appropriate experimental design that integrates all the independent variables and uses the data input from the experiment to find a set of equations that can eventually give the theoretical value of an output. Outputs are obtained by well-designed regression experiments and results from the mathematical model (Shang et al., 2021; Xie et al., 2022; Zhang et al., 2022).

In this study, considering the values specified in the Turkish Ball mill production standard (TS EN 13086 2008) as PbO content (mass fraction) 65-82%, Free Pb content (mass fraction) 18-35%, in this study, PbO (Lead monoxide) was produced in two different metallic lead ratios and its effects on the battery were investigated. In the literature, these ratios are not clearly stated, and it has been observed that the optimum values have changed by considering the raw material and energy losses in production. In the experiments, 25-30% free lead, which is within the standards specified in TS EN 13086 2008, was used.

25% to 30% lead oxide paste was prepared and plastered on the positive plate. Performance experimental studies of the dough on the positive plate were carried out. After the plastering process on the plate, the curing process was performed and SEM and BET analyzes were examined. Capacity, starting, cycle and charge acceptance tests were carried out in the electrical test laboratory, taking into account the TS EN 50342-1 standard. In

addition, by using the response surface method, it was determined that the high efficiency was obtained with 26% lead in the relationship between the lead percentage and the yield, and the yield was inversely proportional with the increase in the lead percentage. It is thought that this situation is due to the effect of particle size and therefore the effect of changing surface area on yield.

## 2. Materials and Methods

In this study, lead monoxide was melted and formed into balls using pure lead with a purity of 99.996%. The balls were then processed in a ball mill to produce two different ratios of lead oxide: 25% Pb-75% PbO (A) and 30% Pb-70% PbO (B). The analysis was performed using the test method specified in the TS EN 13086 standard for lead and lead alloys-lead oxide. The batteries manufactured from the lead monoxide were charged under identical conditions and were subjected to various tests, including capacity, starting, cycle, and charge acceptance tests, as specified in the (TS EN 50342-1 Standard Technical Board, 2016).

### 2.1. Materials Used in Material Synthesis

In this study, the effects of lead oxide produced in lead acid batteries on the battery were investigated. The performance effects of A oxide production and B mixed

oxide production on battery quality were investigated.

Plate dough was prepared from 2 different lead monoxide with ratio A and B. Plastering was done on the positive plate from the prepared dough. These plates were subjected to the curing process under the same conditions and their moisture was removed. 10 batteries (5 A, 5 B batteries) of L2 Type 60 Ah 540 A EN type were made from the plates on the assembly line. The batteries produced on the assembly line were filled with 1.10 gr/cm<sup>3</sup> concentrated sulfuric acid (H<sub>2</sub>SO<sub>4</sub>). The batteries made were charged in the same charging program in the laboratory. After charging, the acid in the batteries was discharged and a new acid with a density of 1.36 gr/cm<sup>3</sup> was added. The batteries were kept for 1 day and capacity tests, starting tests and cycle tests were performed according to the Lead acid accumulators general rules and test methods standard (Chemistry Specialization Group, 2008).

### 2.2. Tests Applied in Material Synthesis

#### 2.2.1. Free lead test in the product after lead oxide production

This test was prepared with reference to the TS EN 13086 standard. 5 g of the oxide sample was weighed and ground in a mortar. After the grinded sample was weighed, it was taken into a flask (Figure 1).



Figure 1. Oxide sample preparation.

Then, 50mL of 20% acetic acid solution was added on it (Figure 2).



Figure 2. Adding solution to the prepared sample.

It was agitated on the heater every 20 seconds until the free lead in the sample precipitated out. 2-3 drops of ascorbic acid were added (Figure 3).

The sample on the blotter was washed first with distilled water and then again with acetone (Figure 4-5).

The sample was placed in an oven with blotting paper and left for 15 minutes. At the end of 15 minutes, the sample was removed from the oven and weighed on a precision balance.



Figure 3. Dissolution of the oxide sample.



Figure 4. Filtration after dissolution.



Figure 5. Washing process after filtration.

### 2.2.2. Weighing process after drying

The % Pb amount was calculated (Equation 1).

$$Pb\% = \frac{(A-B)}{C \times 100} \quad (1)$$

A= Weight of sediment with blotting paper

B= Blotting paper tare

C= Oxide sample weight.

### 2.3. Capacity Test (Ce)

During the whole experiment, the accumulator was kept in a water bath at  $25 \text{ }^\circ\text{C} \pm 2 \text{ }^\circ\text{C}$ . The amount of water in the water bath must be above the battery by a minimum of 15 mm and a maximum of 25 mm. Even if there are multiple batteries, the distance between them should be at least 25 mm and the batteries should be soaked in a water bath for at least 4 hours.

The accumulator must be discharged until the voltage drops to  $10.50 \text{ V} \pm 0.05 \text{ V}$ , keeping the current  $I_n$  at  $\pm 1\%$  of its nominal value. The  $t(h)$  recorded during the discharge time constitutes the capacity time of the battery. The beginning of the discharge should be rested for a period of 1 hour to 5 hours until the end of the charge.

Nominal capacity ( $C_n$ ) = C20 (20 hours capacity, electrical load that can be supplied with current; Ah) shown in the form Equation 1-2.

$$I_n = \frac{C_n}{20} \quad (2)$$

From this formula, the test continues until the final voltage value of the battery is 10.5 V.

$C_e$  = It is the maximum Ah (capacity) value that the battery gives when discharging until it drops to 10.5 V.

The calculated value should be equal to or greater than the declared capacity.

The condition must be Equation 3

$$C_e \geq C_n \quad (3)$$

### 2.4. Starting Test

The charged accumulator should be placed in a circulating cooling chamber at  $-18 \text{ }^\circ\text{C} \pm 1 \text{ }^\circ\text{C}$  until the medium cell temperature reaches  $-18 \text{ }^\circ\text{C} \pm 1 \text{ }^\circ\text{C}$ . It is considered to have reached this temperature after approximately 24 hours.

The accumulator must be discharged with a starting

current ( $I_{cc}$ ) current within 2 minutes after cooling. During discharge, this current should be kept constant within  $\pm 0.5\%$ .

$I_{cc}$  = Starting current (CCA)

After 10 s of discharge, the voltage  $U_f$  between the terminals should be recorded and the current should be cut off.  $U_f$  value should not be less than 7.50 V.

The test should be continued after resting for  $10 \text{ sec} \pm 1 \text{ sec}$ .

The battery should then be re-discharged with a current of  $0.6 I_{cc}$ . During discharge, the current should be kept constant within  $\pm 0.5\%$ . Discharge should be terminated when the battery voltage reaches 6 volts. The discharge time between  $0.6 I_{cc}$  and 6 V is accepted as ( $t'6V$ ) and this time is recorded in seconds.  $t6V$  is defined as the sum of the duration of the second stage ( $t'6V$ ) and the equivalent duration of the first discharge stage (Equation 4.)

$$t6V = t'6V + \frac{10}{0.6} = t'6V + 17 \text{ sec} \quad (4)$$

Condition shown in the form Equation 4-5.

$$t6V > 90 \text{ sec} \quad (5)$$

### 2.5. Cycle Test

The accumulators were connected to a series test circuit and cycled. Each cycle consists of the following two steps: The 1st step battery was discharged for 2 hours with a constant current at  $I = 5 \times I_n$ . The criterion for breaking this test during testing is the voltage at discharge. If it drops below 10.5 V, the test is terminated. In this case, the battery is discharged with 15 Amps for 2 hours. Thus, 30 Ah hours are discharged from the battery (Equation 6-7-8).

$$I_n = \frac{C_n}{20} \quad (6)$$

$$I_n = \frac{60}{20} \quad (7)$$

$$I_n = 3A \quad (8)$$

As a second step, the accumulator is recharged with a constant voltage and a fixed-limited  $5 \times I_n$  current for a maximum of 5 hours. The recharge capacity value is recorded throughout the charge and if it reaches  $CR=1.08$ , the charge is terminated.

Nominal capacity ( $C_n$ ) = C20 (20 hours capacity, current-suppliable electric charge; Ah) (Equation 9).

$$CR = \frac{2Crch}{C_n} \quad (9)$$

$Crch$  = recharge capacity.

If the charging rate CR is lower than 1.08, the battery is

charged with constant current until the CR value in the table is reached, or it is continued until the maximum time reaches 1 hour. In this study, when the determined 60 Ah battery is calculated (Equation10-11),

$$1.08 = \frac{2Crch}{60} \quad (10)$$

$$Crch = 32.4Ah \quad (11)$$

is charged.

After completing step 1 and step 2, this loop represents a cycle. In cycle batteries, these steps are repeated until the voltage limit during discharge is reached or the number of cycles defined in Table 1 is reached. If one of these two conditions is met, the cycle test is completed.

**Table 1.** Cycle classes

Requirement level	Number of cycles
E1	80
E2	150
E3	230
E4	360

### 2.6. Charge Acceptance Test

The accumulator must be discharged at a temperature of 25 °C ± 2 °C for 5 hours with a current I0 (Equation 12),

$$I_0 = \frac{Ce}{10} \quad (12)$$

Ce= It is the maximum Ah (capacity) value that the battery gives when discharging until it drops to 10.5 V.

Within a maximum period of 10 minutes after discharge, the accumulator should be placed in a cooling chamber and cooled until the temperature of its middle cells is 0 °C ± 1 °C. This period should be at least 15 hours.

At this temperature the accumulator is operated with a constant voltage of 14.40 V ± 0.05 V and I<sub>max</sub> = 50 A for batteries with dimensions defined in EN 50342-2 and I<sub>max</sub> = 100 A for batteries with dimensions defined in EN 50342-4 must be charged. According to these conditions, the battery we used in the thesis is classified as I<sub>max</sub>=50 A.

After 10 minutes the charging current I<sub>ca</sub> should be recorded (Equation 13) as a condition.

$$I_{ca} \geq 1I_0 \quad (13)$$

### 2.7. Response Surface Method (RSM)

Experimental data were evaluated using the Surface Response Method (RSM). This method was used in order to obtain maximum efficiency with a minimum of experimental work Uslu and Celik (2020). In this study, when the 2D picture (Figure 6) of the relationship between lead percentage and yield is examined, it is seen that the highest yield is obtained at 26% lead yield and

the yield is inversely proportional with the increase in lead percentage.

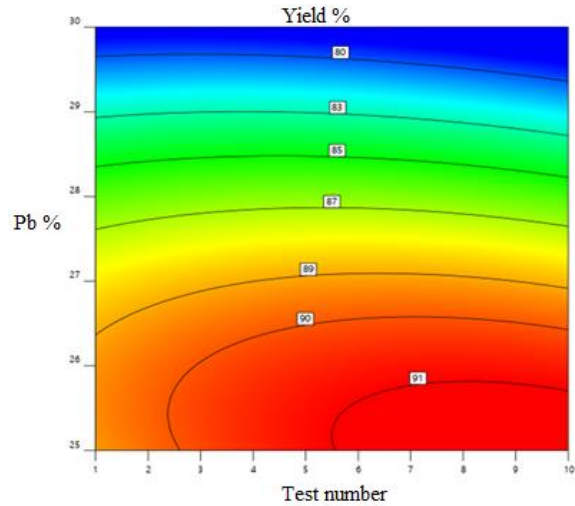


**Figure 6.** Lead percentage and yield graph.

When the 3D Picture (Figure 7-8) is examined, the correctness of the thought behavior is seen. It is seen that the maximum efficiency is in the region containing 26% lead. It is thought that this situation may be due to the effect of particle size and therefore the effect of changing surface area on yield.

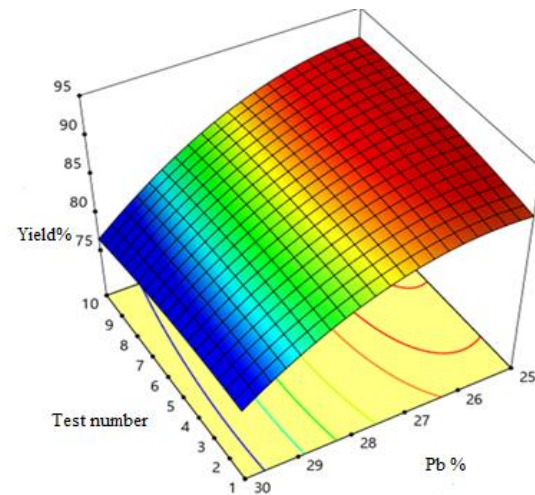


**Figure 7.** Evaluation of experimental data in 3D.

When the normal distribution graph of the residual points is examined, it is seen that there is not much deviation from the linear line. This means that the model is compatible. When the estimated values and the actual value table are examined, deviations from linearity are observed to be negligible. This situation can be interpreted as the result of systematic errors in experimental studies. In addition, the evaluations according to the optimization results are shown in Figure 9.

When the graphs between "Desired" and "Efficiency" are examined, some differences can be seen in the "Desired" graph. These differences are thought to be due to systematic errors (Vahedi et al., 2020).

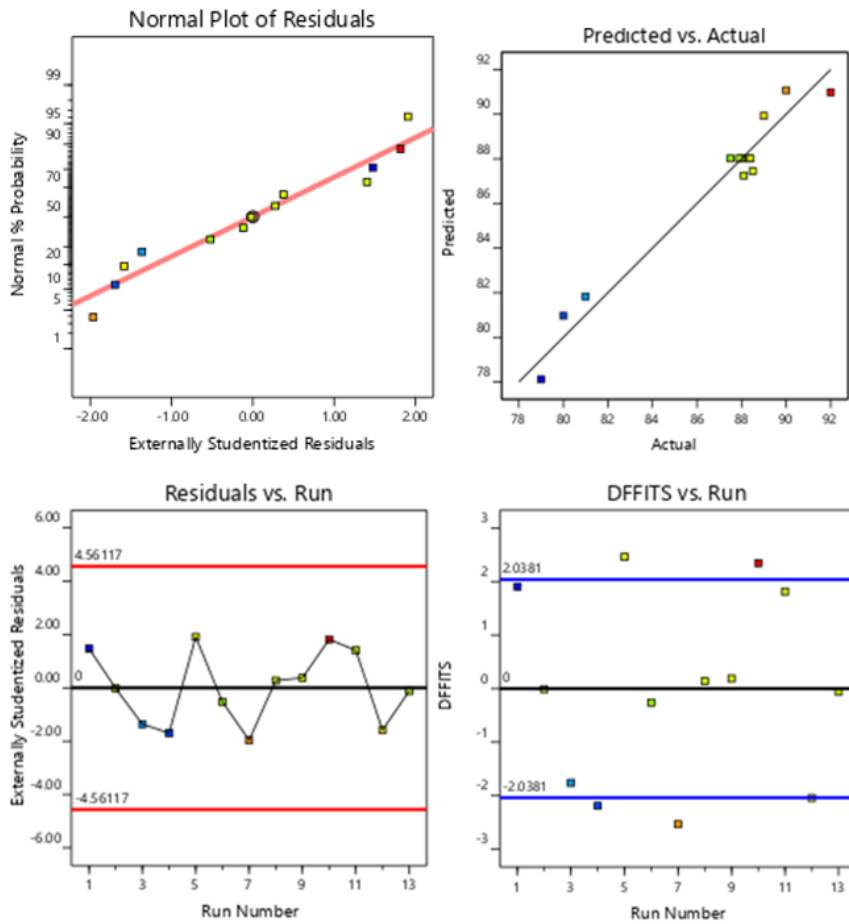


Figure 8. Compatibility of experimental data and model results.

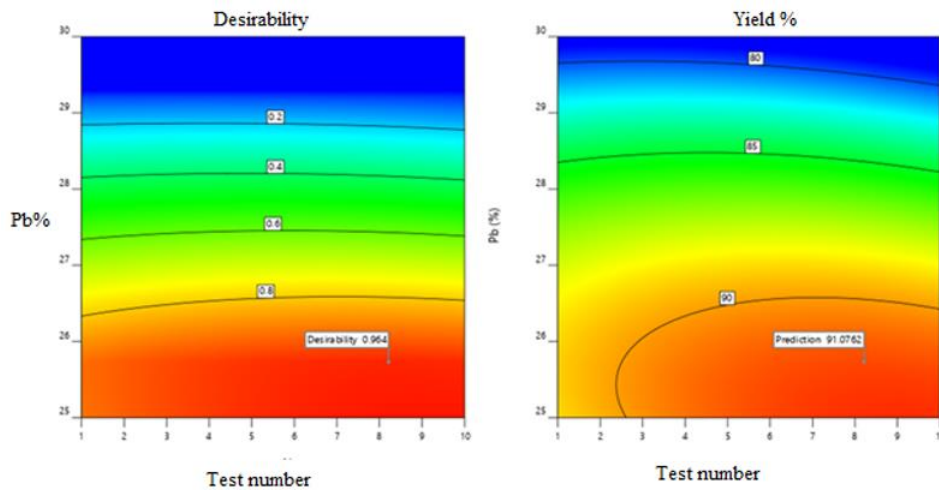


Figure 9. Evaluations according to the optimization results.

Here, a high R<sup>2</sup> value indicates that the results are successful (Table 2).

Table 2. Statistical analysis results

Std. Dev.	1.05	R <sup>2</sup>	0.9601
Mean	86.75	Adjusted R <sup>2</sup>	0.9317
C.V. %	1.22		

$$\text{Yield (\%)} = -275.66575 + 2.83062 \cdot \text{No} + 28.45210 \cdot \text{Pb (\%)} - 0.088889 \cdot \text{No} * \text{Pb (\%)} - 0.033086 \cdot \text{No}^2 - 0.555200 \cdot \text{Pb (\%)}^2 \quad (14)$$

With this obtained equation, it is possible to achieve the desired efficiency when the work is repeated.

When statistical modeling is done, it is seen from the results given in the table above that the Quadratic model is more effective than other models and therefore it is recommended (Table 3).

The model equation found as given in Equation 14,

As can be seen in the analysis table for the Anova Quadratik model, when the model is examined with the 95% confidence interval and the P value of 0.05 as a reference, it is seen that the parameters that are effective

in the specified model are B and B<sup>2</sup>. It is understood that other parameters are not very effective in the specified conditions (Table 4).

**Table 3.** Statistical evaluation

Source	Sum of Squares	df	Mean Square	F-value	P value	
Mean vs Total	97823.64	1	97823.64			
Linear vs Mean	165.52	2	82.76	27.76	<0.0001	
2FI vs Linear	1.0000	1	1.0000	0.3124	0.5899	
Quadratic vs 2FI	21.02	2	10.51	9.45	0.0103	Suggested
Cubic vs Quadratic	0.0585	2	0.0293	0.0189	0.9813	Aliased
Residual	7.73	5	1.55			
Total	98018.97	13	7539.92			

**Table 4.** ANOVA for Quadratic model

Source	Sum of Squares	df	Mean Square	F-value	P value	
Model	187.55	5	37.51	33.72	< 0.0001	significant
A-No	0.0400	1	0.0400	0.0360	0.8550	
B-Pb (%)	165.48	1	165.48	148.77	< 0.0001	
AB	1.0000	1	1.0000	0.8990	0.3746	
A <sup>2</sup>	0.7807	1	0.7807	0.7018	0.4298	
B <sup>2</sup>	20.94	1	20.94	18.83	0.0034	
Residual	7.79	7	1.11			
Lack of Fit	7.28	3	2.43	19.10	0.0078	significant
Pure Error	0.5080	4	0.1270			
Cor Total	195.33	12				

### 3. Results

#### 3.1. Pb% Test in Product after Lead Oxide Production

The products produced in the oxide line were made according to the %Pb test instructions in the product after the lead oxide production according to the TS EN 13086 standard, and results of 25% and 30% were obtained from the results from 2 different production lots. According to this result, batteries were made from these oxides by following the batch.

#### 3.2. Evaluation of Capacity Test Results

The capacity test was carried out to calculate the initial charging efficiency and the effective capacity of the charged batteries. Capacity test was performed on the batteries twice. When the first charge efficiency of the batteries was evaluated according to the results of the 1st capacity test, it was determined that as the amount of free lead of the produced lead oxides decreased, the first charge efficiency was between 88-92%, while the samples with high free lead were between 79-81% (Figure 10).

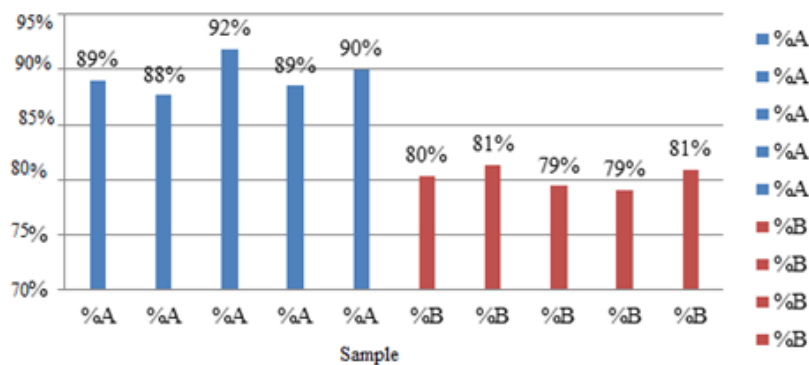


**Figure 10.** Initial charge efficiency graph (25%Pb-75%PbO mix (sample A), 30% Pb-70% PbO (B sample)).



It is believed that the changes in plate morphology during the curing process are the primary reason for this phenomenon, as they affect the initial charge efficiency and charge acceptance of the batteries. During the curing process, the crystals in the dough bond to the plate surface and to each other, resulting in larger crystal structures. Prior to curing, the plate's moisture level was measured at 9%, which decreased to 0.65% after curing. The water particles on the plate surface evaporated during curing, resulting in the formation of stronger structures, including 3BS, 4BS, and PbO structures.

The 3BS structures have a fine particle structure, creating a large surface area, which is an important factor affecting the battery's starting power and charge acceptance. On the other hand, the 4BS structures are coarser and contribute to the battery's cycle life. Due to the high free lead content of the plates undergoing curing, the 4BS ratio was observed to be higher (as shown in Figure 11). The SEM analysis visualized these structures by reducing the size by 10.000  $\mu\text{m}$ .

In this case, it is thought that the plates in the form of 4BS on the right are structurally larger than the plates in the form of 3BS, which increases the internal resistance in the batteries during the charging process. Batteries with high internal resistance can be seen from the maximum temperature value during charging. Since the charge acceptance rate of 3BS structures is higher than 4BS structures, it has been observed that the current given in the 4BS structured batteries increases the reaction temperature without affecting the conversion in the reaction. While the charging temperature of 3BS batteries reaches a maximum of 60 °C (Figure 12). It has found 66 °C in batteries with 4BS. It is also seen from the test results in Figure 12 and Figure 13 that the charge acceptance effect of 3BS structures is more efficient.

In the BET analyzes performed, it was seen that the BET analysis of the A-ratio plate was 1.388  $\text{m}^2/\text{g}$ , while the B-ratio BET analysis was 0.9260  $\text{m}^2/\text{g}$ . In this case, it was observed that the surface area of the samples with A ratio was more than B.

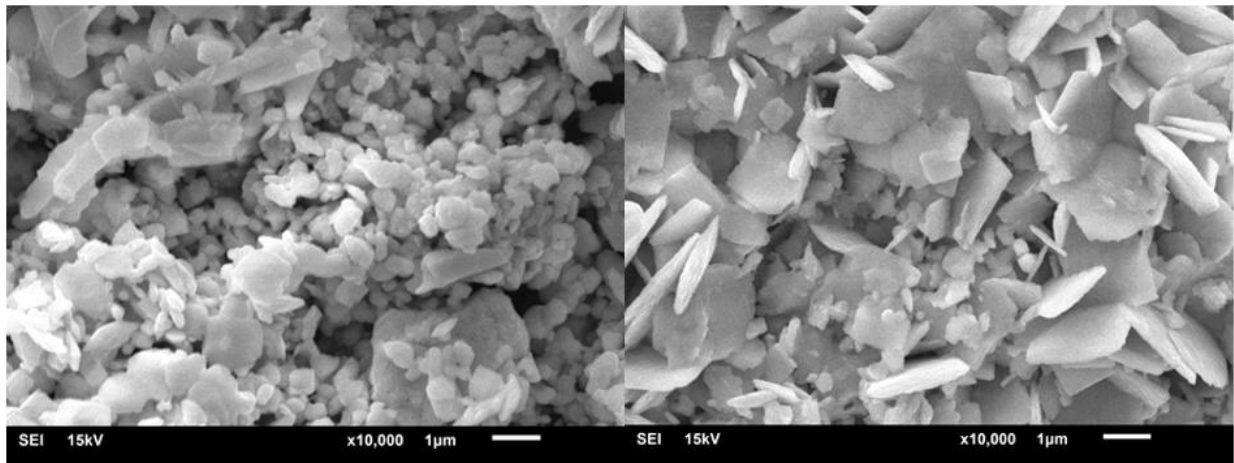


Figure 11. Plate curing manufactured from A, SEM image of end of curing plate made from B SEM image of end.

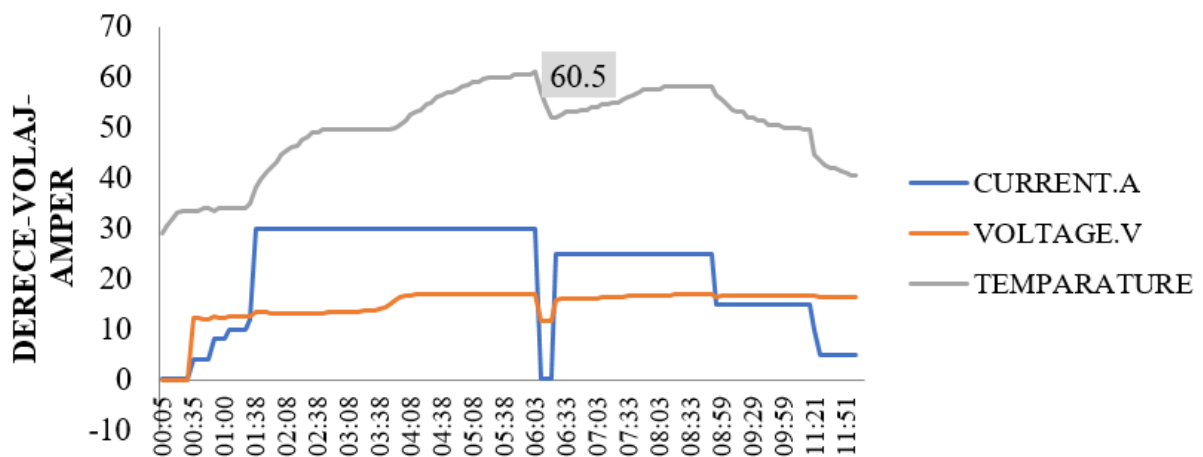


Figure 12. A Sample charge graph (25%Pb-75%PbO mix A sample mix).

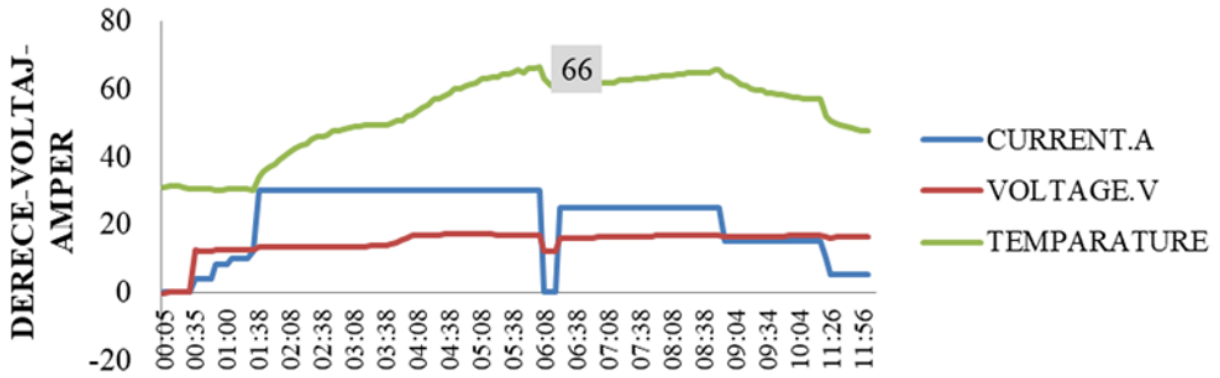


Figure 13. B Sample charge graph (30% Pb-70% PbO (B sample) mix).

3.3. Evaluation of Start Test Results

This test was carried out according to the test instruction specified in the TS EN 50342-1 standard. The purpose of this test is to determine the starting power of the batteries. When the tests were performed according to the standard, no positive or negative effect of both conditions on the starting power was observed in the results. It is seen that the effect is not much in the results obtained (Figure 14).

A test was conducted following the TS EN 50342-1 standard to determine the cycle life of the batteries by measuring the number of charge-discharge cycles. The impact of 3BS and 4BS structures on the battery performance was also investigated in this study while examining the previous capacity test. It was anticipated that 3BS structures with smaller particle size would have a shorter cycle life due to quicker spillage compared to 4BS structures with larger particles. However, if there is no spillage, the battery with better charge acceptance is expected to perform more efficiently in the cycle. The results of the test showed that batteries made from A-rated plates completed 180 cycles, while B-rated

batteries completed 165 cycles (Figure 15).

3.4. Evaluation of Charge Acceptance Test Results

This test was carried out according to the test instruction specified in the TS EN 50342-1 standard. The purpose of this test is to measure the charging capability of the batteries after deep discharge. Since the current value given to the fully discharged batteries is charged in the constant current constant voltage method, the current value will start to decrease when the voltage value reaches the limit. When the current values taken after 10 minutes were compared during this period, it was seen that sample A received 18.45 A current, while sample B received 11.04 A current. This indicated that the charge acceptance of sample A was higher (Figure 16). When the result is evaluated according to the TS EN 50342-1 standard;

$$I_0 = 60/10$$

$$I_0 = 6 \text{ Amper}$$

Conditions (Equation 15)

$$I_{ca} \geq 2I_0 \tag{15}$$

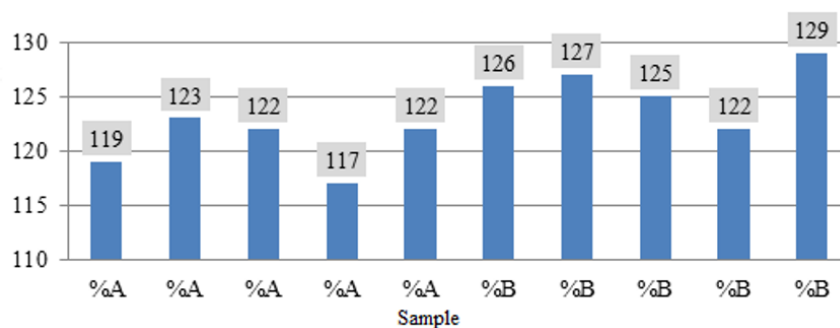


Figure 14. Starting performance test result t6 volt duration condition>90 seconds evaluation of cycle test results(25%Pb-75%PbO mix (A sample) , 30% Pb-70% PbO (B sample) mix).

4. Discussion

This study aimed to investigate the impact of lead oxide production on lead acid battery quality. Specifically, the effects of two different ratios of lead oxide production (25% Pb-75% PbO and 30% Pb-70% PbO) on battery performance were evaluated. As the oxidized lead ratio increased in the lead oxide production, it was observed that the plates contained more 3BS structures after the

curing process, with smaller crystal structures in samples with low oxidized lead content. In terms of charge acceptance, it was observed that the batteries with 3BS structures had higher charge acceptance. The first charge efficiency of samples with high lead oxide content was around 90% on average, while those with low lead oxide content remained at 80%. Additionally, samples with higher charge acceptance cycled more.

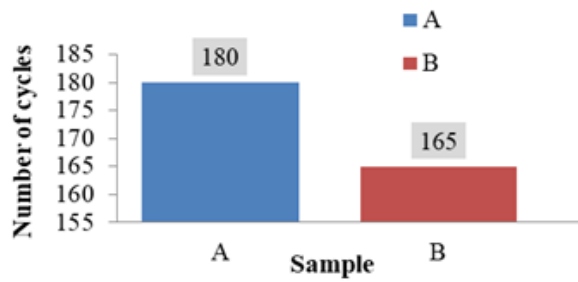


Figure 15. Cycle test result (25%Pb-75%PbO mix (A sample), 30% Pb-70% PbO (B sample) mix).

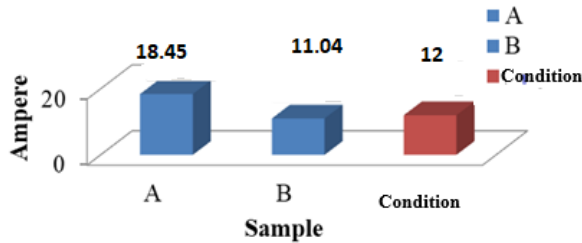


Figure 16. Charge acceptance test result (25%Pb-75%PbO mix (A sample), 30% Pb-70% PbO (B sample) mix).

Sample A was found to be 12% more effective in initial charging efficiency than sample B, 67% more efficient in charge acceptance tests, and 6.5% more efficient in cycle tests. Furthermore, it was observed that the initial charge efficiency, charge acceptance, and cycle life decreased as the %Pb ratio in the lead oxide product increased. The relationship between lead percentage and yield was analyzed using the response surface method, revealing that the highest yield was obtained at a 26% lead yield, with the yield being inversely proportional to the increase in lead percentage due to the effect of particle size and changing surface area.

### Author Contributions

The percentage of the author(s) contributions is presented below. All authors reviewed and approved the final version of the manuscript.

	E.P.	Z.G.Y.
C	40	60
D	40	60
S	30	70
DCP	60	40
DAI	40	60
L	50	50
W	20	80
CR	20	80
SR	20	80
PM	40	60
FA	40	60

C=Concept, D= design, S= supervision, DCP= data collection and/or processing, DAI= data analysis and/or interpretation, L= literature search, W= writing, CR= critical review, SR= submission and revision, PM= project management, FA= funding acquisition.

### Conflict of Interest

The authors declared that there is no conflict of interest.

### Ethical Consideration

Ethics committee approval was not required for this study because of there was no study on animals or humans.

### Acknowledgements

In this department, Emrah Pıçakçı, a graduate student and working at Ako Battery Factory, conducted experiments at the factory. Her advisor, Zehra Gülten Yalçın, carried out the studies of designing the experiments, reviewing the literature, applying the RSM model and writing the article by interpreting it. SEM and BET analyzes were performed at Çankırı Karatekin University. We thank the Ako Battery Factory Authorities in Çankırı for providing laboratory facilities in the study.

### References

- Arun S, Kiran KUV, Mayavan S. 2020. Effects of carbon surface area and morphology on performance of stationary lead acid battery. *J Energy Stor*, 32: 101763.
- Bao J, Lin N, Dan Y, Gao W, Liu Z, Lin H. 2021. Anodic co-electrodeposition of hierarchical porous nano-SiO<sub>2</sub>+ PbO<sub>2</sub> composite for enhanced performance of advanced lead-carbon batteries. *J Energy Stor*, 35: 102285.
- Bode H. 1977. *Lead-acid Batteries, Handbook of Batteries*, 3rd ed. John Wiley & Sons Inc., Hoboken, US.
- Bode H. 1979. Lead-acid batteries. *J Power Sour*, 4(3): 252-255.
- Chen T, Huang H, Ma H, Kong D. 2013. Effects of surface morphology of nanostructured PbO<sub>2</sub> thin films on their electrochemical properties. *Electrochimica Acta*, 88: 79-85.
- Chemistry Specialization Group. 2008. Lead and lead alloys-Lead oxides. TS EN 13086, April 4, 2008.
- Dayton TC, Edwards DB. 2000. Improving the performance of a high power, lead-acid battery with paste additives. *J Power Sour*, 85(1): 137-144.

- Draper NR, Pukelsheim F. 1996. An overview of design of experiments. *Stat Papers*, 37: 1-32.
- Elkelawy M, El Shenawy EA, Bastawissi HAE, Shams MM, Panchal H. 2022. A comprehensive review on the effects of diesel/biofuel blends with nanofluid additives on compression ignition engine by response surface methodology. *Energy Convers Manag*: X: 100177.
- Eydemir Y. 2019. Strengthened battery design in start-stop vehicles. MSc Thesis, Gazi University, Faculty of Technology, Energy Systems Engineering, Ankara, Türkiye, pp: 93.
- Garche J. 1990. On the historical development of the lead/acid battery, especially in Europe. *J Power Sour*, 31(1-4): 401-406.
- Gutiérrez AS, Eras JJC, Santos VS, Herrera HH, Hens L, Vandecasteele C. 2018. Electricity management in the production of lead-acid batteries: The industrial case of a production plant in Colombia. *J Clean Prod*, 198: 1443-1458.
- Jensen WA. 2017. Response surface methodology: process and product optimization using designed experiments. *J Quality Technol*, 49(2): 186.
- Jia X, Liu C, Neale ZG, Yang J, Cao G. 2020. Active materials for aqueous zinc ion batteries: synthesis, crystal structure, morphology, and electrochemistry. *Chemical Rev*, 120(15): 7795-7866.
- Karimi MA, Karami H, Mahdipour M. 2006. Sodium sulfate as an efficient additive of negative paste for lead-acid batteries. *J Power Sour*, 160(2): 1414-1419.
- Kocakulak T, Halis S, Ardebili SMS, Babagiray M, Haşimoğlu C, Rabeti M, Calam A. 2023. Predictive modelling and optimization of performance and emissions of an auto-ignited heavy naphtha/n-heptane fueled HCCI engine using RSM. *Fuel*, 333: 126519.
- Kwiecien M, Badeda J, Huck M, Komut K, Duman D, Sauer DU. 2018. Determination of SoH of lead-acid batteries by electrochemical impedance spectroscopy. *Appl Sci*, 8(6): 873.
- Lach J, Wróbel K, Wróbel J, Podsadni P, Czerwiński A. 2019. Applications of carbon in lead-acid batteries: a review. *J Solid State Electrochem*, 23: 693-705.
- Liu J, Yang D, Gao L, Zhu X, Li L, Yang J. 2011. Effect of iron doped lead oxide on the performance of lead acid batteries. *J Power Sour*, 196(20): 8802-8808.
- Lu Y, Zhao CZ, Yuan H, Hu JK, Huang JQ, Zhang Q. 2022. Dry electrode technology, the rising star in solid-state battery industrialization. *Matter*, 5(3): 876-898.
- Mayer MG, Rand DAJ. 1996. Lead oxide for lead/acid battery positive plates: scope for improvement?. *J Power Sour*, 59(1-2): 17-24.
- Mitchell P, Zhong L, Xi X, Zou B. 2009. Dry particle based adhesive and dry film and methods of making same. US7508651.
- Pavlov D. 2011. Lead-acid batteries: science and technology. Elsevier, New York, US, pp: 707.
- Pıçakçı E, Yalçın ZG, Dağ M, Aydoğmuş E. 2021. The Effects of Using High Rate Lead (II) Oxide(PBO) on Battery. *EasyChair Preprint* № 692. URL: [https://easychair.org/publications/preprint\\_download/Lrkj](https://easychair.org/publications/preprint_download/Lrkj) [accessed date: February 10, 2023].
- Sagbas A. 2022. Analysis and optimization of process parameters in wire electrical discharge machining based on RSM: A case study. In *Response Surface Methodology- Research Advances and Applications*. IntechOpen, DOI: 10.5772/intechopen.102317.
- Shang L, Yan Y, Zhan Y, Ke X, Shao Y, Liu Y, Lin M. 2021. A regulatory network involving Rpo, Gac and RSM for nitrogen-fixing biofilm formation by *Pseudomonas stutzeri*. *NPJ Biofilms Microbiomes*, 7(1): 54.
- Tong P, Zhao R, Zhang R, Yi F, Shi G, Li A, Chen H. 2015. Characterization of lead (II)-containing activated carbon and its excellent performance of extending lead-acid battery cycle life for high-rate partial-state-of-charge operation. *J Power Sour*, 286: 91-102.
- Technical Board. 2016. Lead-acid starter batteries-Part 1: General requirements and methods of test. TS EN 50342-1.
- Uslu S, Celik MB. 2020. Performance and exhaust emission prediction of a SI engine fueled with I-amyl alcohol-gasoline blends: an ANN coupled RSM based optimization. *Fuel*, 265: 116922.
- Vahedi Torshizi M, Azadbakht M, Kashaninejad M. 2020. A study on the energy and exergy of Ohmic heating (OH) process of sour orange juice using an artificial neural network (ANN) and response surface methodology (RSM). *Food Sci Nutrit*, 8(8): 4432-4445.
- Wang J, Li M, Hu J, Ke Y, Yu W, Wang Z, Yang J. 2020. Effect of particle size on phase transitions of positive active materials made from novel lead oxide during soaking process and its influence on lead-acid battery capacity. *J Energy Stor*, 28: 101175.
- Wang S, Xia B, Yin G, Shi P. 1995. Effects of additives on the discharge behaviour of positive electrodes in lead/acid batteries. *J Power Sour*, 55(1): 47-52.
- Xie L, Zhou Y, Xiao S, Miao X, Murzataev A, Kong D, Wang L. 2022. Research on basalt fiber reinforced phosphogypsum-based composites based on single factor test and RSM test. *Construct Build Mater*, 316: 126084.
- Yang W, Gao Z, Ma J, Wang J, Wang B, Liu L. 2013. Effects of solvent on the morphology of nanostructured Co<sub>3</sub>O<sub>4</sub> and its application for high-performance supercapacitors. *Electrochimica Acta*, 112: 378-385.
- Yin J, Lin Z, Liu D, Wang C, Lin H, Zhang W. 2019. Effect of polyvinyl alcohol/nano-carbon colloid on the electrochemical performance of negative plates of lead acid battery. *J Electroanalytical Chem*, 832: 152-157.
- Zhang FY, Zhou HY, Yuan JQ, Li QH, Diaoyu YW, Zhang LJ, Du L. 2022. Optimization of nitrosation reaction for synthesis of 4-aminoantipyrine by response surface methodology and its reaction mechanism. *Organic Proces Res Devel*, 26(11): 3051-3066.
- Zhang K, Liu W, Ma B, Mezaal MA, Li G, Zhang R, Lei L. 2016. Lead sulfate used as the positive active material of lead acid batteries. *J Solid State Electrochem*, 20: 2267-2273.
- Zhang WL, Yin J, Lin ZQ, Shi J, Wang C, Liu DB, Lin HB. 2017. Lead-carbon electrode designed for renewable energy storage with superior performance in partial state of charge operation. *J Power Sour*, 342: 183-191.